CHEMICAL ENGINEERING TRANSACTIONS

VOL. 94, 2022

A publication of AIDIC

The Italian Association of Chemical Engineering
Online at www.cetjournal.it

Guest Editors: Petar S. Varbanov, Yee Van Fan, Jiří J. Klemeš, Sandro Nižetić

**ISBN** 978-88-95608-93-8; **ISSN** 2283-9216

DOI: 10.3303/CET2294011

# Mapping the Thermohydraulic Performance of Turbulence Promoters

Leidy Paola Durán-Plazas, Martín Picón-Núñez*, Jesús Isaac Minchaca-Mojica

University of Guanajuato, Department of Chemical Engineering, Noria Alta s/n, Guanajuato, Guanajuato, C.P. 36050. Mexico
picon@ugto.mx

As a result of the wide use of tubular heat exchangers in industry and considering the main heat transfer and friction limitations they possess compared to new technologies, heat transfer promoters of different shapes have appeared in recent years to improve their thermohydraulic performance. To date, there are many different promoter geometries each with its heat transfer and friction performance. This situation makes the selection of the right promoter for retrofit applications a complex task. To overcome this situation, this paper provides a performance mapping plot for the identification of the best promoter geometries out of the many available. This work demonstrates that it is possible to identify the promoters that best perform out of the many geometries available in applications at low and high-pressure drops. To this end, an arbitrarily selected group of different turbulence promoters are compared in terms of measurable parameters such as heat load and pressure drop. Besides, the results are confirmed using thermal and pressure drop irreversibility analysis. Different selection criteria can be applied based on the allowable pressure drop. In the case of retrofit, the best performance is identified by increased heat load for the same installed area with the lowest increment on pressure drop compared to the base case.

## 1. Introduction

Turbulence promoters are a suitable tool in the retrofit of existing tubular heat exchangers. These devices increase the heat duty without modifying the dimensions of the unit. An accompanying effect when using inserts is an increase in drop pressure. The increase in both heat duty and drop pressure is specific to each insert and their relationship is different from one promoter to another. Since for a given case many different types of promoters can be used, knowledge of their thermohydraulic performance is essential for selection purposes. In the open literature, many studies that address the performance comparison of turbulence promoters can be found. For example, the performance criterion method (RC) (García et al., 2007), the thermal performance factor ($\eta$) (Eiamsa-Ard and Promvonge, 2011), the thermal performance factor based on an identical flow rate, JF (Dang and Wang, 2021), the dimensionless number, Fc, also referred to as the field synergy number (Yu et al., 2020), the performance evaluation criterion, PEC (Mousa et al., 2021) and the Figure of Merit (FoM) that is calculated in the same manner as the PEC and combines the benefit of heat transfer enhancement with the penalty of higher pressure drop (Tusar et al., 2021). In other studies, the concept of entropy was used to evaluate the thermodynamic performance of turbulence promoters. Among these studies are Zimparov and Penchev (2006) that used the entropy generation number, Ns, and the work by Chaurasia and Sarviya (2021) that extended the entropy generation minimization method. In terms of performance comparison methods for different promoters, Durán-Plazas et al. (2021) used a thermal length and hydraulic length model as an alternative approach for the selection of tube inserts when a given application is considered. With their approach, they provided a quick comparison method of the thermo-hydraulic performance of different turbulence promoters in both design and retrofit applications. The above review indicates that there is a scope for further research in terms of finding the most suitable promoter for a given application since several factors must be taken into consideration. For instance, it is important to know how much heat load increase is desirable and what is the

Paper Received: 15 April 2022; Revised: 27 April 2022; Accepted: 02 May 2022
Please cite this article as: Durán-Plazas L.P., Picón-Núñez M., Minchaca-Mojica J.L., 2022, Mapping the Thermohydraulic Performance of Turbulence Promoters, Chemical Engineering Transactions, 94, 67-72 DOI:10.3303/CET2294011

maximum additional pressure drop the system can withstand. This work introduces a simple approach to answer this question for single phase heat transfer applications. The approach consists of a plot where the performance of the available promoters is compared using the new-to-base case heat load ratio vs the new-to-base case pressure drop ratio. It is also shown that the results are confirmed using a plot of the heat transfer and pressure drop irreversibility. A group of turbulence promoters selected arbitrarily out of the many that have been published, are used to demonstrate the methodology.

## 2. Heat exchanger retrofit

In retrofit applications of existing single phase heat exchangers, a convenient way of assessing the suitability of a turbulence promoter is to determine the new outlet temperatures for the improved heat transfer coefficients. This can be achieved in a simple manner using the thermal effectiveness-number of heat transfer units. The thermal effectiveness (ε) is the ratio of the actual heat load to the maximum duty that is thermodynamically possible. This term can be represented by the ratio of the temperature change of the $CP_{min}$ to the maximum temperature driving force in the exchanger given by the difference between the hot and cold inlet temperatures. $CP_{min}$ is the lowest product between the heat capacity and the mass flow rate of the two streams. Considering the operating temperatures for a case where the hot stream is the $CP_{min}$ stream, the thermal effectiveness of the exchanger can be expressed as:

$$\varepsilon = (T_1 - T_2)/(T_1 - T_3) \tag{1}$$

Where $T_1$ and $T_3$ are the hot and cold inlet temperatures and $T_2$ and $T_4$ are the hot and cold outlet temperatures. For a heat exchanger in counter-current arrangement ($\varepsilon$) can be expressed as:

$$\varepsilon = (1 - e^{-[-Ntu*(1-C)]})/(1 - C * e^{-[-Ntu*(1-C)]}) \tag{2}$$

When the exchanger has multiple tube passes, the expression is:

$$\varepsilon = 2/\{(1 + C) + (1 + C^2)^{1/2}[(1 + e^{-Ntu*(1+C^2)^{1/2}})/1 - e^{-Ntu*(1+C^2)^{1/2}}]\} \tag{3}$$

Where *Ntu* and *C* are the number of heat transfer units and the ratio $CP_{min}/CP_{max}$ and are defined as:

$$Ntu = U A/CP_{min} \tag{4}$$

$$C = CP_{min}/CP_{max} \tag{5}$$

Where U is the overall heat transfer coefficient (W/m$^2$°C), and A is the exchanger surface area (m$^2$).

$$1/U = 1/h_1 A + 1/h_2 + R_k + R_f \tag{6}$$

The implementation of a turbulence promoter inside a tube increases the heat transfer coefficient which in turn increase the overall heat transfer coefficient and Ntu. The thermal effectiveness is changed and its new value can be calculated from Eq(2) or Eq(3) depending on the exchanger design. The new cold stream outlet temperature ($T_4$) is determined from Eq(1) and then the outlet temperature for the hot side ($T_2$) is calculated form:

$$CP_{min}(T_1 - T_2) = CP_{min}(T_4 - T_3) \tag{7}$$

In this work it is assumed that the Reynolds number does not vary significantly with the implementation of the promoter. Therefore, the Reynolds number is calculated from:

$$Re = \dot{m}\, d_i/A_c\, \mu \tag{8}$$

Where $\dot{m}$ is the mass flow rate (kg/s), $d_i$ is the inner tube diameter (m), $A_c$ is the tube side free flow area (m$^2$) and $\mu$ the fluid viscosity (kg/m s). Considering the total number of tubes ($N_t$), the free flow area on the tube side can be calculated from:

$$A_c = \pi\ N_t\, d_i{}^2/4 \tag{9}$$

Where $N_t$ is the number of tubes and $d_i$ is the tube inner diameter (m). The new heat exchanger heat load can be calculated form:

$$Q = CP_{min}(T_1 - T_4) \tag{10}$$

The pressure drop of the exchanger can be calculated from:

$$\Delta P = \rho f L_t v_t{}^2/2d_i \tag{11}$$

Where $v_t$ is the tube side fluid velocity (m/s), $f$ is the friction factor (-), $L_t$ is the tube length (m), $\rho$ is the density (kg/m$^3$). For the analysis 12 different tube inserts are analysed. The expression that represent their thermohydraulic performance are shown in Figure 1.

| No. | Type | Geometrical Parameter | Nusselt number | Friction factor |
|---|---|---|---|---|
| 0 | Smooth tube | - | $Nu = 0.023Re^{0.8}Pr^{0.4}$ | $f = 0.184Re^{-0.2}$ |
| 1 | Perforated twisted tape (Bhuiya et al., 2013) | $R_p$ = 1.6, 4.5, 8.9, 14.7% | $Nu = (0.0002R^3 - 0.0046R^2 + 0.0334R\ ppp + 0.6569).Re^{(0.00005R^3 - 0.0013R^2 + 0.0073R + 0.5501)}Pr^{0.3}$ | $f = (-0.0027R^3 + 0.0583R^2\ pp + 0.0455R_p + 24.536).Re^{(0.00005R^3 - 0.0022R^2 + 0.012R - 0.6006)}$ |
| 2 | TT inserts placed separately from the tube wall (Bas and Ozceyhan, 2012) | y/D = 2.0, 2.5, 3.0, 3.5, 4.0 c/D = 0.0178, 0.0357 | $Nu = 0.406903Re^{0.586556}Pr^{0.38}(y/D)^{-0.443989}(c/D)^{-0.055072}$ | $f = 0.406903Re^{0.45085}(y/D)^{-0.730772}(c/D)^{-0.1579}$ |
| 3 | Quadruple perforated-delta-winglet pairs (PW-XT). (Skullong et al., 2016) | $B_R$ = 0.1, 0.15, 0.2, 0.25 $P_R$ = 0.5, 1.0, 1.5, 2.0 | $Nu = 0.194Re^{0.777}Pr^{0.4}B^{0.317}P^{-0.373}$ | $f = 5.305Re^{-0.076}B^{0.976}P^{-0.989}$ |
| 4 | Straight tape with center wings (T-W) and F-wings (Eiamsa-ard and Promvonge, 2011) | $e_p$ = 0.75, 1.0, 1.25 $e_w$ = 0.5, 0.67, 0.83 | $Nu = 0.112Re^{0.731}Pr^{0.4}(e_p)^{-0.283}(e_w)^{0.316}$ | $f = 1.55Re^{-0.138}(e_p)^{-0.635}(e_w)^{0.759}$ |
| 5 | Inclined horseshoe baffles 45 (Promvonge et al., 2014) | $B_R$ = 0.1, 0.15, 0.2 $P_R$ = 0.5, 1.0, 2.0 | $Nu = 0.1944Re^{0.7381}Pr^{0.4}B^{0.2264}P^{-0.1454\ RR}$ | $f = 12.979Re^{-0.1228}B^{1.5282}P^{-0.4735\ RR}$ |
| 6 | Twisted cross- baffles (Nanan et al., 2016) | P/D = 1.0, 1.5, 2.0 | $Nu = 0.093Re\ Pr^{0.4}(p/D)^{-0.403}$ | $f = 0.093Re^{-0.096}(p/D)^{-1.036}$ |
| 7 | Alternate twisted-baffles (Nanan et al., 2016) | P/D = 1.0, 1.5, 2.0 | $Nu = 0.075Re^{0.799}Pr^{0.4}(p/D)^{-0.249}$ | $f = 0.895Re^{-0.093}(p/D)^{-0.669}$ |
| 8 | Equilateral triangular cross sectioned CW. (Keklikcioglu, Ozceyhan, 2017) | P/D = 1, 2, 3 e/D = 0.0714, 0.0892 | $Nu = 0.515Re^{0.584}Pr^{0.39}(P/D)^{-0.334}(e/D)^{0.11}$ | $f = 72.599Re^{-0.514}(P/D)^{0.367}(e/D)^{0.486}$ |
| 9 | CW placed separately. (Gunes et al., 2010) | P/D = 1, 2, 3 e/D = 0.0714, 0.0892 | $Nu = 0.07715Re^{0.71692}Pr^{0.4}(P/D)^{-0.253417}(S/D)^{-0.124382}$ | $f = 3.970492Re^{-0.367485}(P/D)^{-0.31182}(S/D)^{-0.157719}$ |
| 10 | Circular-rings and twisted tapes (Eiamsa-ard et al., 2013) | y/W = 3, 4, 5 l/Di = 1, 1.5, 2 | $Nu = 0.326Re^{0.724}Pr^{0.4}(l/D)^{-0.475}(y/w)^{-0.406}$ | $f = 13.99Re^{0-202}(l/D)^{-0927}(y/w)^{-0.619}$ |
| 11 | Regulary spaced quadruple twisted tapes in co arrangement (Co-RS-QTT) (Simruaisin et al., 2018) | s/y = 0.5, 1.0, 1.5, 2.0 | $Nu = 0.152Re^{0.678}(s/y)^{-0.039}Pr^{0.4}$ | $f = 1.458Re^{0.222}(s/y)^{-0.052}$ |
| 12 | Regulary spaced quadruple twisted tapes cross arrangement (Cross-RS-QTT) (Simruaisin et al., 2018) | s/y = 0.5, 1.0, 1.5, 2.0 | $Nu = 0.565Re^{0.543}(S/Y)^{-0.053}Pr^{0.4}$ | $f = 1.93Re^{-0.24}(S/Y)^{-0.041}$ |

*Figure 1: Thermohydraulic performance of the selected heat transfer promoters*

## 3. Irreversibility

Irreversibility measures the lost opportunity of producing work. In a heat exchanger, it manifests in two ways: by the existence of temperature gradients for heat transfer and by the losses created due to friction. In a retrofit project using turbulence promoters, the purpose is to increase the heat load of the exchanger which in terms of temperature gradients means to reduce them by increasing the heat removal capacity. In terms of irreversibility, this results in lower irreversibility loss. On the hydraulic side, the use of turbulence promoters always results in an increase of pressure drop which translates in the increase of irreversibility. Therefore, what is desirable in the performance of a turbulence promoter is the maximum reduction in the irreversibility due to heat transfer and the lower increase in irreversibility due to pressure drop. The irreversibility can be computed from the entropy generation as:

$$Irreversibility = \dot{s}_{gen}T_0 \tag{12}$$

Where $\dot{s}_{gen}$ is the entropy generated (W/K) and $T_0$ is the ambient temperature. The entropy generated due to heat transfer ($\dot{s}_{gen,h}$) is:

$$\dot{s}_{gen,h} = (\dot{m}Cp)_h ln\frac{T_{h,out}}{T_{h,in}} + (\dot{m}Cp)_c ln\frac{T_{c,out}}{T_{c,in}} \tag{13}$$

Where $(\dot{m}Cp)_h$ and $(\dot{m}Cp)_c$ are the mass flow rate (kg/s) and heat capacity (J/kg K) of the hot and cold streams, $T_{h,in}$ and $T_{h,out}$ are the hot stream inlet and outlet temperature (K), $T_{c,in}$ and $T_{c,out}$ are the cold stream inlet and outlet temperature. The entropy generated due to pressure drop is calculated from:

$$\dot{s}_{gen,f} = \frac{1}{T_c}\ \frac{\dot{m}_c}{\rho_c}\Delta P_c + \frac{1}{T_h}\ \frac{\dot{m}_h}{\rho_h}\Delta P_h \qquad (14)$$

Where $\rho_c$ and $\rho_h$ are the density of the cold and hot fluids; $\Delta P_c$ (Pa) and $\Delta P_h$ (Pa) are the pressure drop on the cold and hot sides and $T_c$ and $T_h$ are the average temperature of the cold and cold fluids. The procedure for the calculation of the heat load, pressure drop, and irreversibility is illustrated in Figure 2.

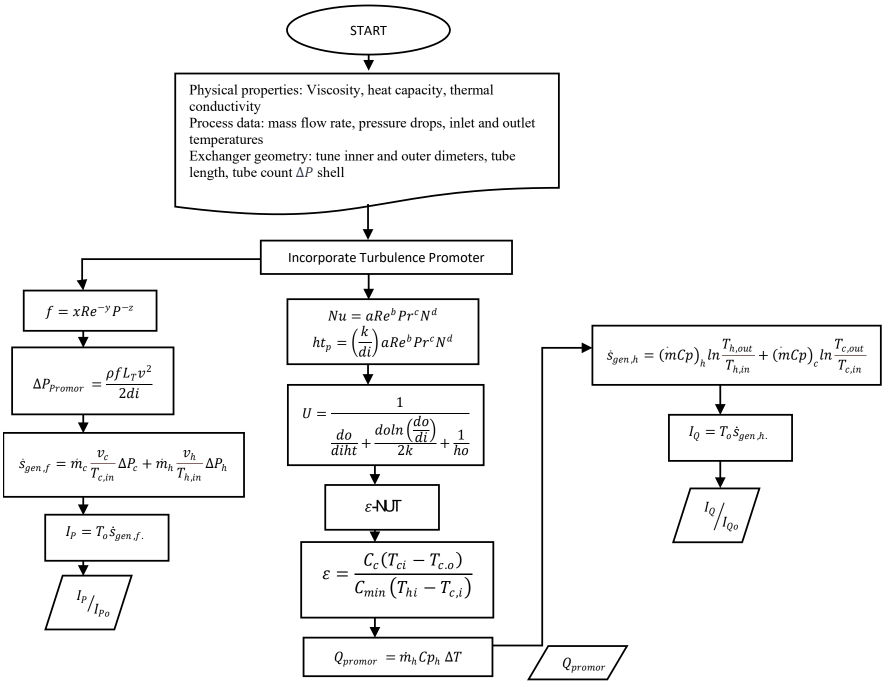


*Figure 2: Flow chart of the computation of new thermal and pressure drop of a heat exchanger with turbulence promoters*

## 4. Case studies

In this section, three case studies are analysed where three existing heat exchangers are retrofitted to increase its heat load. For each case, the thermal and pressure drop performance ratio are plotted to generate the performance mapping plot. Cases 1 and 2 are used to demonstrate that for the same working fluid, the relative position of the promoters in the map does not change with the Reynolds number, but the relative increment of heat duty and pressure drop does change. Case study 3 is used to show that the relative position of the promoters is modified depending on the type of fluid being used. Thus, the selection of the best heat transfer promoter depends on the specific application. Figure 3 shows the physical properties, operating conditions, and exchanger geometry of the three cases.

| | **Case 1** | | **Case 2** | | **Case 3** | |
|---|---|---|---|---|---|---|
| | **Tube side** | **Shell side** | **Tube side** | **Shell side** | **Tube side** | **Shell side** |
| Heat load (kW) | 2,889.6 | | 2,889.6 | | 2,883 | |
| Heat transfer area ($m^2$) | 322.67 | | 174.91 | | 331.42 | |
| Overall heat transfer coefficient (W/$m^2$°C) | 358.21 | | 660.8 | | 347.96 | |
| Mass flow (kg/s) | 68.8 | 13 | 68.8 | 13 | 100 | 12 |
| Tin (°C) | 25 | 95 | 25 | 95 | 25 | 95 |
| Tout (°C) | 40 | 40 | 40 | 40 | 40 | 40 |
| Heat capacity (J/kg °C) | 2.8 | 4.2 | 2.8 | 4.2 | 1.9 | 4.2 |
| Density (kg/$m^3$) | 750 | 995 | 750 | 995 | 882 | 995 |
| Viscosity (kg/ m $s^2$) | 3.40E-04 | 8.00E-04 | 3.40E-04 | 8.00E-04 | 5.27E-03 | 8.00E-04 |
| Thermal conductivity (W/m°C) | 0.19 | 0.59 | 0.19 | 0.59 | 0.289 | 0.59 |
| Pressure drop (Pa) | 147.4 | 1,760.6 | 3,091.4 | 26,462.4 | 7,513 | 4730 |
| Reynolds number | 9,406 | 2,258 | 34,704 | 6,880 | 8,805 | 8931 |
| Heat transfer coefficient (W/$m^2$ °C) | 785.2 | 1,856.2 | 2,231 | 3,426 | 704 | 1318 |
| External diameter (m) | 0.02 | | 0.02 | | 0.06 | |
| Thickness (m) | 0.002 | | 0.002 | | 0.002 | |
| Internal diameter (m) | 0.016 | | 0.016 | | 0.056 | |
| Tube length (m) | 1.5 | | 3 | | 9 | |
| Pt pitch triangular (m) | 0.025 | | 0.025 | | 0.075 | |
| Number of tubes | 3,424 | | 928 | | 190 | |
| Tube passes | 2 | | 2 | | 4 | |
| Thermal conductivity of material (W/m°C) | 50 | | 50 | | 50 | |

*Figure 3: Process data and physical properties of the case studies 1, 2 and 3*

Figure 4 shows the performance mapping for case study 1. Figure 4a corresponds to a design where the tube side pressure drop is low (147.4 Pa). Under these conditions, the following scenarios can be analysed. Since the pressure drop is small, then an increment of up to 22 times (see maximum increment in Figure 1a) will allow to choose the promoter that delivers the highest heat duty increment. This is promoter No. 3 that increases heat duty in approximately 7.5 %. The pressure drop increment is 12.5 times resulting in a new pressure drop of 1,837.5 Pa which is still a low pressure drop that may not cause pumping problems. These results are corroborated in Figure 4b where promoter No. 3 exhibits the lowest thermal irreversibility ratio. Figure 5a shows the performance mapping of case study 2 where the same problem is analysed but with a different exchanger geometry with a higher pressure drop. In this case, the pressure drop on the tube side is 3,091.4 Pa. Such pressure drop indicates that only small increments of pressure drop can be tolerated otherwise the pumping system can be compromised. Assuming a maximum pressure drop increase of 5 times, Figure 5a reveals that promoter No. 1 gives the largest heat load increment of about 4 %. Figure 5b shows the results for case study 3 where a case with a higher viscosity fluid is analysed. As seen in Figure 5b, the performance mapping shows that the promoters have a similar relative position. If only small increases in pressure drop can be accepted, promoter No.1 would be the choice.

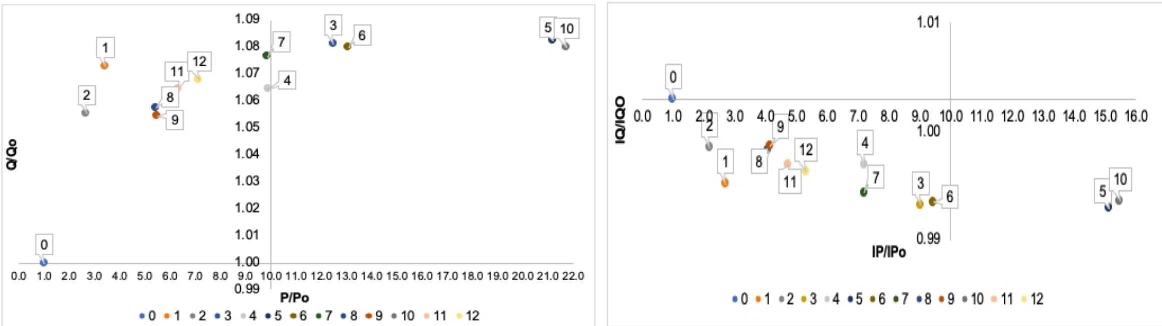


a) b)

*Figure 4: Turbulence promoter performance mapping for case study 1: a) Relative heat load vs relative pressure drop, b) Relative irreversibility due heat load vs relative irreversibility due to pressure drop.*

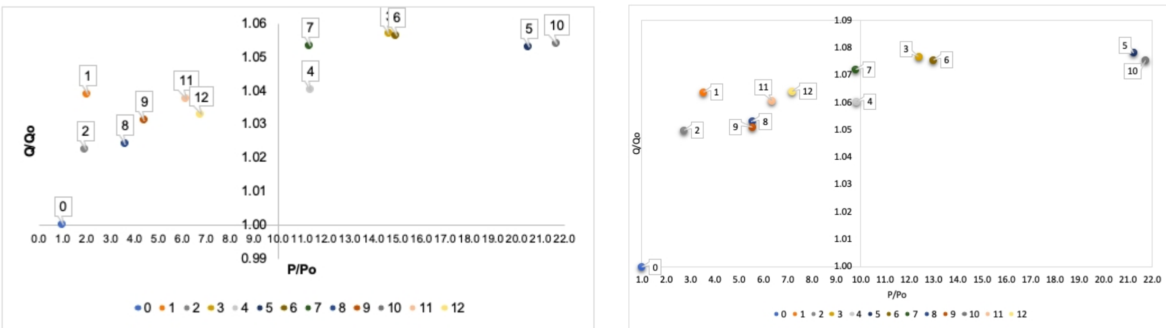


a) b)

*Figure 5: Turbulence promoter performance mapping: a) Case study 2, b) Case study 3.*

## 5. Conclusions

The main conclusions of this work are:

- Thermohydraulic performance mapping is a practical means of identifying the best turbulence promoter to use in retrofit applications.
- The choice of the most suitable promoter for a given application depends on the required increment on heat duty and the maximum pressure drop increment that can be accepted.
- The options to choose from are wider in problems operating at low-pressure drops.
- For a practical selection of the right turbulence promoter, the whole exchanger performance must be analysed. Comparison of the single tube side heat transfer enhancement may give only a partial view of the problem. Performance mapping gives a complete view of the exchanger enhanced performance.
- The relative performance of turbulence promoters seems to be unchanged with the type of problem which is determined by the tube side physical properties, Reynolds number and pressure drop. This

indicates that once the criteria is set (required increment in heat duty and maximum permitted pressure drop) the best performing promoters will always be the same.
- Work is underway to include new turbulence promoters in the analysis.

**References**

Bas H., Ozceyhan V., 2012, Heat transfer enhancement in a tube with twisted tape inserts placed separately from the tube wall. Experimental Thermal and Fluid Science, 41, 51-58.

Bhuiya M. M. K., Chowdhury M. S. U., Saha M., Islam M. T., 2013, Heat transfer and friction factor characteristics in turbulent flow through a tube fitted with perforated twisted tape inserts. International Communications in Heat and Mass Transfer, 46, 49-57.

Chaurasia S. R., Sarviya R. M., 2021, Comparative thermal performance analysis with entropy generation on helical screw insert in tube with number of strips with nanofluid at laminar flow regime, International Communications in Heat and Mass Transfer, 122, 105138.

Dang W., Wang L. B., 2021, Convective heat transfer enhancement mechanisms in circular tube inserted with a type of twined coil, International Journal of Heat and Mass Transfer, 169, 120960.

Durán-Plazas L.P., Picón-Núñez M., Minchaca-Mojica J.I., 2021, Selection of heat transfer promoters for heat exchanger retrofit, Chemical Engineering Transactions, 88, 523-528.

Eiamsa-ard S., Kongkaitpaiboon V., Nanan K., 2013, Thermohydraulics of turbulent flow through heat exchanger tubes fitted with circular-rings and twisted tapes. Chinese Journal of Chemical Engineering, 21(6), 585-593.

Eiamsa-Ard S., Promvonge P., 2011, Influence of double-sided delta-wing tape insert with alternate-axes on flow and heat transfer characteristics in a heat exchanger tube, Chinese Journal of Chemical Engineering, 19(3), 410-423.

García A., Solano J. P., Vicente P. G., Viedma A., 2007, Enhancement of laminar and transitional flow heat transfer in tubes by means of wire coil inserts, International Journal of Heat and Mass Transfer, 50(15-16):3176–3189.

Gunes S., Ozceyhan V., Buyukalaca O., 2010, Heat transfer enhancement in a tube with equilateral triangle cross sectioned coiled wire inserts. Experimental Thermal and Fluid Science, 34(6), 684-691.

Keklikcioglu O., Ozceyhan V., 2017, Entropy generation analysis for a circular tube with equilateral triangle cross sectioned coiled-wire inserts. Energy, 139, 65-75.

Mousa M. H., Miljkovic N., Nawaz K., 2021, Review of heat transfer enhancement techniques for single phase flows, Renewable and Sustainable Energy Reviews, 137, 110566.

Nanan K., Piriyarungrod N., Thianpong C., Wongcharee K., Eiamsa-ard S., 2016, Numerical and experimental investigations of heat transfer enhancement in circular tubes with transverse twisted baffles. Heat and Mass Transfer, 52(10), 2177-2192.

Promvonge P., Suwannapan S., Pimsarn M., Thianpong C., 2014, Experimental study on heat transfer in square duct with combinedtwisted-tape and winglet vortex generators, International Communications in Heat and Mass Transfer, 59, 158-165.

Simruaisin P., Changcharoen W., Thianpong C., Chuwattanakul V., Pimsarn M., Eiamsa-Ard S., 2018, Influence of regularly spaced quadruple twisted tape elements on thermal enhancement characteristics. Chemical Engineering and Processing-Process Intensification, 128, 114-123.

Skullong S., Promvonge P., Thianpong C., Pimsarn M., 2016, Thermal performance in solar air heater channel with combined wavy-groove and perforated-delta wing vortex generators, Applied Thermal Engineering, 100,611-620.

Tusar M.H., Bhowmik P.K., Salam B., Ahamed J.U. and Kim J.K., 2021, Convective heat transfer and friction factor characteristics of helical strip inserted annuli at turbulent flow, International Journal of Heat and Mass Transfer, 176, 121422.

Yu C., Zhang, H., Wang, Y., Zeng, M., Gao, B., 2020, Numerical study on turbulent heat transfer performance of twisted oval tube with different cross sectioned wire coil. Case Studies in Thermal Engineering, 22, 100759.

Zimparov V.D. and Penchev P.J., 2006, Performance evaluation of some tube inserts as heat transfer enhancement techniques, Heat Transfer Engineering, 27, 8:39-46.